The effect of vehicle on skin absorption of Mg2+ and Ca2+ from thermal spring water

Malgorzata Tarnowska, S. Briancon, Jacqueline Resende de Azevedo, Yves Chevalier, Delphine Arquier, C. Barratier, M.-A. Bolzinger

The effect of vehicle on skin absorption of Mg^{2+} and Ca^{2+} from Thermal Spring Water

Małgorzata Tarnowska, Stéphanie Briançon, Jacqueline Resende de Azevedo, Yves Chevalier, Delphine Arquier, Cynthia Barratier, Marie-Alexandrine Bolzinger*

Univ Lyon, Université Claude Bernard Lyon 1, CNRS, LAGEPP UMR 5007, Laboratoire de Dermopharmacie et Cosmétologie, Faculté de Pharmacie de Lyon, 43 bd 11 Novembre 1918, 69622 Villeurbanne, France.

*Corresponding Author:

Marie-Alexandrine Bolzinger

Tel: +(33) 4 78 77 71 12

Fax: +(33) 4 78 78 56 47

E-mail: marie.bolzinger@univ-lyon1.fr

Authors' E-mails:

malgorzata_tarnowska@hotmail.com; Tel: +(33) 4 72 43 18 94

stephanie.briancon@univ-lyon1.fr; Tel: +(33) 4 72 43 18 45

jacqueline.resende-de-azevedo@univ-lyon1.fr; Tel: +(33) 4 78 77 71 36

yves.chevalier@univ-lyon1.fr; Tel: +(33) 4 72 43 18 77

delphine.arquier@univ-lyon1.fr; Tel: +(33) 4 78 77 71 15

cynthia.barratier@univ-lyon1.fr; Tel: +(33) 4 78 77 71 35

marie.bolzinger@univ-lyon1.fr; Tel: (+33) 4 78 77 70 21

Keywords: Skin barrier; Emulsions; Delivery/vectorization/penetration; Liposomes; Thermal Spring Water; Franz cell

Data included in the manuscript were presented during Skin Forum 23rd and 24th September 2019, Reims, France and partially during Formulation Days - Advances in Formulation of Active Ingredients, Lyon, January 10th and 11th 2019.

Abstract

OBJECTIVE: Thermal spring waters (TSW) are commonly used as active ingredients in cosmetics. Their biological activities directly depend on the ionic composition of the spring. However, in order to exhibit beneficial properties, the minerals need to reach viable skin layers. The present study addresses the incorporation of marketed TSW in model cosmetic formulations and the impact of the formulation on skin absorption of magnesium and calcium ions that are known to improve skin barrier function.

METHODS: Marketed TSW was introduced into 5 formulations. Liposomes were prepared using saturated or unsaturated phospholipids mixed with cholesterol by the thin layer evaporation technique. Emulsions (water-in-oil, oil-in-water or double: water-in-oil-in-water) were prepared by high shear mixing. Skin absorption of Mg^{2+} and Ca^{2+} from those formulations was studied *in vitro* using static Franz diffusion cells.

RESULTS: Mg^{2+} and Ca^{2+} penetrate skin samples from TSW. Encapsulating TSW into double emulsion (TSW/O/W) increased skin absorption of both cations of interest and kept the Ca^{2+}/Mg^{2+} ratio equal to that of TSW in each skin layer. The dermal absorption of Mg^{2+} from the double emulsion departs from both single emulsions. Application of liposome suspension improved the skin absorption of Ca^{2+} while keeping constant that of Mg^{2+}, leading to unbalanced Ca^{2+}/Mg^{2+} ratio inside skin.

CONCLUSION: The beneficial effects of TSW are not only due to their action on the skin surface. Their active components, especially Ca^{2+} and Mg^{2+} cations reach viable skin layers in a formulation-dependent manner. The distribution of ions inside skin depends on the type of formulation.

Introduction

Curative properties of thermal spring waters (TSW) have been known and used in treatment of various skin (psoriasis, eczema etc.) and systemic diseases (ex. osteoarthritis, mental stress, sleep disorders) since many centuries [1, 2]. “Taking the waters” is the most ancient water treatment which is “promising relief to the sick”, as written by Elder Pliny in the book XXXI of his Natural History and reported by Jackson [3]. Water cures are very common and strongly embedded in European cultures (France, Italy, Germany, Hungary). The core of balneotherapy has been defined by Gutenbrunner as the “use for natural mineral waters, gases and peloids (including packs that are local applications of peloids), often in resorts (Spas)” which are located next to the sea (Dead-Sea) or thermal sources in European countries [4,5]. The therapeutic use of mineral waters sourced from trapped oceanic waters (Dead Sea, Tiberias waters) and other locations, like Vichy water in France, has been evaluated as beneficial by the Cochrane Library. Such an adjuvant treatment is recommended for dermatologic and rheumatologic diseases, and also for patients with all forms of arthritis [6–8]. A 3-week spa therapy has prolonged, beneficial, symptomatic effects against osteoarthritis that were maintained for more than 6 months [8].

All TSW contain significant amount of magnesium, calcium, and sulfate ions [9]. It is presently questioned whether the components of TSW are able to cross hydrophobic barrier of *stratum corneum* and reach viable layers of epidermis and dermis. Several authors have addressed the permeability of skin for ions, both *in vitro* [10–12] and in clinical trials [13, 14], demonstrating that dermal and even transdermal delivery of ions is indeed possible under certain conditions.

Among cations of interest, Ca^{2+} and Mg^{2+} have been recognized for their benefits in skin barrier recovery [15]. High concentrations of endogenous Ca^{2+} and Mg^{2+} are present in the uppermost epidermis. They are distributed according to a concentration gradient increasing in the epidermis from the *stratum basale* up to the *stratum granulosum*. In case of external damage,

this gradient is perturbed which is a signal for skin barrier repair driven by lipids exocytosis from lamellar bodies [16–20]. Denda *et al*. reported that application of ionomycin, a calcium ionophore, in cultured human keratinocytes delayed the barrier repair by increasing the intracellular calcium concentration. In their *in vivo* study on rats exposed to ionomycin, the authors showed that the lipid domains at the *stratum corneum-stratum granulosum* interface were relatively thin and skins contained many unsecreted lipids inside lamellar bodies [19]. Another study disclosed the effects of mixed magnesium and calcium salts with varying molar ratio [15]. Salt solutions having Mg^{2+} to Ca^{2+} ratio higher than 1 accelerate barrier recovery in a more efficient way than solutions of each cation separately. The solution of $CaCl_2$ (10 mM) alone delays recovery of *stratum corneum* in mice. Dietary recommendations encourage daily intake of calcium and magnesium in a ratio close to 2, which disagrees with the findings of Denda *et al*., who recommended an inverted molar ratio (Mg^{2+}:Ca^{2+} > 1) for acceleration of skin barrier recovery. Magnesium and probably calcium mainly permeate through skin by the follicular pathway [12]. However, the absorption profiles of these cations applied together as in the case of TSW are not documented. Moreover, “encapsulation” in various vehicles may modulate the distribution of both ions, thereby modifying the Ca^{2+}:Mg^{2+} molar ratio that controls lipids release from lamellar bodies.

Calcium- and magnesium-rich TSW are known to improve skin barrier function, accelerate wound healing [20, 21] and have soothing and protective properties for sensitive skin (antioxidant or anti-ageing) together with trace elements such as selenium, strontium and zinc [22–24]. These properties have been demonstrated in many studies using human keratinocytes, fibroblasts or other response-appropriate cell lines [6, 25, 26]. Therefore, they are considered as active substances when used in a cosmetic product. TSW in spray form may cause secondary skin dehydration. Evaporation of TSW at the skin surface increases osmotic pressure and leads to crystallization of salts that cause greater water loss from deep skin layers and skin dryness in

general. Therefore, TSW-based skin care products are developed to overcome the drawbacks of a simple spray form, allowing incorporation of other types of active cosmetic ingredients in one product. As discussed by Otto *et al.*, dermal delivery of molecules depends strongly not only on their physicochemical properties, but also on the formulation in which it is incorporated [27]. Though several TSW-based cosmetic formulations have been claimed, no skin absorption of ions from such products has been reported so far. In this study using the Franz cell method, we investigated the dermal penetration of TSW rich in Ca^{2+} and Mg^{2+} entrapped in different formulations: classical emulsions, double emulsions and, liposomes. Liposomes are known to enhance skin permeation of entrapped drugs and improve skin repair [28, 29]. Moreover, phospholipids containing high amounts of phosphatidylcholine (> 90%) promote penetration into epidermis by altering the barrier properties of the lipid medium of the *stratum corneum* [30]. W/O/W multiple emulsions are composed of both W/O and O/W droplets. The oil phase makes a barrier between both aqueous phases and may lead to a sustained release of the cations from the internal water droplets as reported by Ferreira *et al.* for glucose, a highly hydrophilic ingredient [31]. Additionally, multiple emulsions may stabilize active ingredients and contribute to a better skin hydration [32].

Materials and Methods

Chemicals

Marketed, mixed sulfate-chloride thermal spring water was purchased at a local pharmacy. Medium chain triglycerides (MCT, Labrafac Lipophile WL 1349) were kindly provided by Gattefossé, France. Polyglyceryl-4-polyricinoleate (PGPR, Dermofeel PGPR®) was a generous gift from Evonik, France. Glyceryl Citrate/Lactate/Linoleate/Oleate (G-CLLO, IMWITOR®375) was obtained from IOI Oleo GmbH, Germany. Hydrogenated phosphatidylcholine (> 90%) (Phospholipon® 90H) and pure phosphatidylcholine (> 94%) (Phospholipon® 90G) were kind gifts

from Lipoid GmbH, Germany. Cholesterol, Certified Multielement Ion Chromatography Anion Standard Solution, Certified Multielement Ion Chromatography Cation Standard Solution, nitric acid (HNO_3) and dipicolinic acid were from Sigma Aldrich, France. Betaine (trimethylglycine), sodium hydrogen carbonate ($NaHCO_3$), sodium carbonate (Na_2CO_3), sodium dihydrogen phosphate (NaH_2PO_4), potassium dihydrogen phosphate (KH_2PO_4) and glucose were purchased from Acros Organics, France. Ultrapure water with resistivity > 18 MΩ·cm at 25 °C was used in all experiments.

TSW physicochemical characterization

The composition of the TSW marketed product has been measured by ionic chromatography (Table I). Analysis has been restricted to ions of interest. Traces of oligo elements such as zinc and strontium reported as components by the supplier have not been quantified in the present study.

Controls of osmolality, pH, conductivity, and dry residue were performed. Osmolality and pH were evaluated using and Osmomat 030 (Cryoscopic osmometer, Gantec, Berlin, Germany) and a pH-meter (pHenomenal® pH, VWR equipped with an electrode pH 11769798, Fisher Scientific, France) respectively. Conductivity was measured using a Conductivity Meter (CDM210, MeterLab®). The mineralisation level was evaluated by gravimetric analysis after evaporation of water from 10 mL TSW using a rotary evaporator (200 mbar, 70 °C, Rotavapor® R-205, Büchi, Switzerland).

Table I. Characterisation of TSW. Values in standard font are given according to the supplier, values in *italics* are the present measurements.

Parameters		**Mineral content (mmol·L^{-1})**			
Spring water temperature (°C)	- 62	**Cations**		**Anions**	
Dry residue (g·L^{-1})	*6.86* 6.72	Li^+	*0.14* -	F^-	*0.11* 0.11
Conductivity at 25 °C (mS·cm^{-1})	*9* -	Na^+	*69.8* 75.2	Cl^-	*87.7* 56.9
Osmolality (mOsm·kg^{-1})	*180* "isotonic against skin cells"	K^+	*3.40* 3.46	Br^-	*0.09* 0.02
pH	*5.5* 7.04	Mg^{2+}	*4.36* 3.50	NO_3^-	*0.04* > 0.01
Ca^{2+}:Mg^{2+}Mole ratio	*3:1* 3:1	Ca^{2+}	*13.4* 10.3	SO_4^{2-}	*31.3* 22.6

Formulations

The compositions of formulations (Table II) were designed so that the final concentrations of Mg^{2+} and Ca^{2+} in each formulation were kept constant. There was no other source of Mg^{2+} and Ca^{2+} (nor other ions) in the formulations. Classical TSW/O and O/TSW emulsions contained 60% *m/m* of TSW. O/TSW emulsion was prepared by the heat-heat process: TSW containing G-CLLO and oil were heated up to 60 °C; both phases were mixed with an IKA T25 digital Ultra-Turrax® at 20,000 rpm and then cooled down to room temperature. TSW/O emulsion was prepared at room temperature by mixing the oil and aqueous phases using an IKA T25 digital Ultra-Turrax® at 20,000 rpm for 5 min. The PGPR hydrophobic surfactant was incorporated in the oil phase.

The composition of TSW/O/W emulsion was based on the TSW/O primary emulsion. TSW/O/W double emulsions were prepared at room temperature using a two-step method. In the first step, TSW/O was prepared as described above. The TSW used in the formulation was concentrated twice using a rotary evaporator (200 mbar, 70 °C, Rotavapor® R-205, Büchi, Switzerland) and filtered through 0.45 µm syringe filters (WhatmanTM Uniflo) prior to use to

ensure the same concentration of calcium and magnesium in the final formulation. This procedure led to an increase in osmolality of TSW from 180 to 360 mOsm·kg^{-1}. In order to avoid instability of double emulsion (over-swelling due to differences in osmotic pressure), betaine (300 mmol·kg^{-1}) was added to the continuous phase containing G-CLLO (hydrophilic surfactant) as an osmotic agent that does not change ionic strength of the solution. In the second step, the primary emulsion was dispersed in the external aqueous phase using an IKA T25 digital Ultra-Turrax® at 5,000 rpm for 1 min. Two liposome suspensions containing 60% (m/m) TSW were prepared by the thin lipid film hydration method [33] using saturated (LPM-90H) or unsaturated (LPM-90G) phospholipids. Saturated (Phospholipon® 90H) or unsaturated (Phospholipon® 90G) phospholipids and cholesterol were solubilized in 15 mL of mixture of chloroform, diethyl ether and methanol (7:7:1, *v/v/v*). Evaporation of the organic solvents under vacuum (300 mbar, 60 °C) led to the thin lipid layer formation. TSW (diluted for the final concentration of 60%) was used to rehydrate the lipids. Then, the dispersion was vortexed for 5 min and warmed in a water bath at 60 °C for 5 min. The cycle was repeated three times and led to the formation of primary suspension of multilamellar liposomes. It was then sonicated using an ultrasonic disperser Sonics VibraCell equipped with a 25 mm shaft working at 20 kHz, 500 W power and 40 % of the full amplitude (Bioblock Scientific, France) for 12 min with ice cooling.

Table II. Composition of the formulations. Values are given as % *m/m* of the final preparation. Asterisk (*) refers to the percentage of double-concentrated TSW used in the formulation. Theoretical contents of Mg and Ca were 2.7 and 8.0 mmol·kg^{-1} respectively.

EMULSIONS					LIPOSOMES		
Components	**O/TSW**	**TSW/O**	**TSW/O/W**		**Components**	**90H (saturated)**	**90G (unsaturated)**
TSW	60	60	60*	50 %	**Phospholipid**	2.5	2.5
MCT	35	35	35	primary	**Cholesterol**	0.5	0.5
PGPR	0	5	5	TSW/O	**TSW (60%)**	97	97
G-CLLO	5	0	0	5			
H_2O isotonic	0	0	0	45			

Physicochemical characterizations

Size (*z*-average diameter) and width of size distribution (*PDI*) of liposomes were measured by means of dynamic light scattering (Malvern Zetasizer Nano ZS®). Samples were diluted with ultrapure water prior to measurements and analysed at 25 °C at a scattering angle of 173°. pH was measured on fresh formulations.

Droplet size range in emulsions O/TSW, TSW/O and TSW/O/W was assessed from diluted samples by optical microscopy imaging using 100-fold magnification of the objective (Leica DM LM, France).

Liposomes were observed by means of Cryogenic-transmission electron microscopy (Cryo-TEM) at the "Centre Technologique des Microstructures" (CTμ, http://microscopies.univ-lyon1.fr/ facility of the University of Lyon 1). Liposomes were deposited onto 300 mesh holey carbon films (Quantifoil R2/1) and quench-frozen in liquid ethane using a cryo-plunge workstation (made at Laboratoire de Physique des Solides, Orsay, France). Prepared samples were then mounted on a precooled Gatan 626 specimen holder, transferred in the microscope (Philips CM120) and observed at an accelerating voltage of 120 kV.

Viscosity of emulsions was measured at 25 °C using MRC 302 Rheometer (Anton Paar, France) 24 h after preparation using a cone–plate measuring device of 25 mm diameter, at the shear strain rate of 300 s^{-1}.

pH was verified for the formulations with aqueous continuous phase (LPM-90H, LPM-90G, O/TSW and TSW/O/W) using pH-meter (pHenomenal® pH, VWR equipped with an electrode pH 11769798, Fisher Scientific, France).

Skin absorption

Skin samples preparation

Flank skin excised from young female pigs (32 ± 2 kg) sacrificed at Léon Bérard Medical Centre (Lyon, France), was used as a model for human skin given the similarities between these species in terms of *stratum corneum* and full skin thickness, hair follicle density as well as ion composition [34–36]. Freshly excised tissue samples were used immediately after harvesting (< 1 h). The subcutaneous adipose tissues were carefully removed with a scalpel to yield a final thickness of 1.29 ± 0.02 mm (Micrometer Mitutoyo) and cut into round sections of 3 cm^2. Skin integrity was checked by measuring the Trans Epidermal Water Loss (TEWL; Tewameter TM210, Monaderm, Monaco). Samples having TEWL values above 15 $g \cdot h^{-1} \cdot m^{-2}$ after 1 min were discarded. The average TEWL value of skin samples used for experiments was 11.0 ± 0.3 $g \cdot h^{-1} \cdot m^{-2}$.

Skin absorption study and Ca^{2+} and Mg^{2+} distribution after 24 h

Skin absorption studies were performed in static diffusion cells according to OECD guidelines [37]. Full-thickness, freshly excised skin samples were mounted in two-chamber Franz glass cells (exposure area 2.54 cm^2) with the *stratum corneum* facing the donor chamber.

1 g of freshly prepared formulation (LPM-90H, LPM-90G, TSW/O, O/TSW, TSW/O/W) and TSW (60%) as a control containing 1.0 $\mu mol \cdot cm^{-2}$ Mg^{2+} and 3.2 $\mu mol \cdot cm^{-2}$ Ca^{2+} was deposited on the

skin surface. The acceptor compartment was filled with 10 mL of the survival medium designed to provide high metabolic activity of the skin samples during experiments. It was isotonic against skin cells (betaine 250 mmol·L^{-1}) but contained the minimal amount of ions so that its composition did not interfere with the experimental setup. Glucose (1 g·L^{-1}) provided the energetic fuel for skin cells and phosphate buffer ensured physiological pH over the exposure to formulations [38].

Franz cells were placed in a water bath at 37 °C with magnetic stirring so that the surface of skin was 32 °C after heat loss. After 24 h exposure under occlusive conditions, the cells were dismantled. The non-absorbed fraction was removed from the skin surface by washing the donor chamber thrice with 1% solution of the polyethylene glycol *tert*-octylphenyl ether Octoxynol-9 nonionic surfactant (Triton X-100; Sigma Aldrich, France). The glass donor chamber and the skin surface were then whipped carefully with cellulose tissue paper. Next, skin layers were separated as follows: *stratum corneum* (SC) was removed using cyanoacrylate glue (Loctite SuperGlue-3, Henkel) spread on a glass plate. The viable epidermis (VE) was separated from the dermis (D) by heat treatment (45 s in water at 60 °C). The ions were extracted from the cellulose whip paper and each skin layer by sonication for 30 min at 60 Hz followed by extraction overnight (17 h) in water/dichloromethane (1:1 *v/v*) mixture under magnetic stirring [36]. The addition of the organic solvent, which is not soluble in water and has higher density than water, allowed easier separation of aqueous phase from the lipidic fraction extracted from the emulsions and skin samples. Recovered quantity of ions was quantified by ion chromatography for the donor solution, acceptor medium (AM) and different skin layers after filtration of the aqueous fractions of samples through 0.45 µm syringe filters (Whatman™ Uniflo). The amount extracted from the whip paper was added to that of the donor solution, yielding the amount of the donor compartment (DC). The mass balance calculations indicated the recovery of 100 ± 15 % of initially applied dose proving that the extraction method allowed complete ion recovery.

The full absorbed recovered amount (Q_{abs}) corresponded to the sum of the recovered amounts in SC, VE, D and AM. For each experiment, $n \geq 8$ replications were performed. Blank experiments were carried on simultaneously on skin samples of each donor to assess the amounts of endogenous Ca^{2+} and Mg^{2+}. The donor chamber was left empty and rinsing step while dismantling the cells was skipped. The rest of manipulations were performed as described for skin absorption studies. The amounts of Ca^{2+} and Mg^{2+} eluted to AM and recovered inside skin layers after 24 h were quantified by ion chromatography and subtracted from the experimental values of samples, so that only the exogenous fraction was considered.

Ion chromatography

Ion contents of TSW, blank and formulation-exposed skin samples together with AM and DC were evaluated using ion chromatography (930 Compact IC Flex, Metrohm, Switzerland).

Anions were analysed at 35 °C using Metrosep A Supp 5 250/4.0 column with an adapted pre-column (Metrosep A Supp 5 Guard/4.0). Standard eluent (1.0 $mmol \cdot L^{-1}$ $NaHCO_3$ and 3.2 $mmol \cdot L^{-1}$ Na_2CO_3) was used.

Cation analysis of TSW samples was performed using Metrosep C6 250/4.0 column with an adequate pre-column (Metrosep C 6 Guard/4.0) at the temperature of 45 °C. Mobile phase was 1.7 $mmol \cdot L^{-1}$ HNO_3; and 1.7 $mmol \cdot L^{-1}$ dipicolinic acid.

Injection volume of 20 µL was used for the analyses of TSW. Calibration curves measured by diluting Certified Multielement Ion Chromatography Anion Standard Solution (10.0 $mg \cdot kg^{-1}$ ± 0.2% of each anion: F^-, Cl^-, Br^-, NO_3^-, PO_4^{3-}, SO_4^{2-}) and Certified Multielement Ion Chromatography Cation Standard Solution (10.0 $mg \cdot kg^{-1}$ ± 0.2% of each cation: Li^+, Na^+, K^+, Mg^{2+}, Ca^{2+}) were linear in the range from 0.25 to 10.0 $mg \cdot kg^{-1}$ for both cations and anions ($R^2 = 0.999$). For analyses of samples from skin absorption experiments (DC, SC, VE, D, AM) a higher concentration of the eluent was used (2.27 $mmol \cdot L^{-1}$ HNO_3 and 2.27 $mmol \cdot L^{-1}$ dipicolinic acid)

and the injection volume was 100 µL. The calibration curve from a mixture of $MgSO_4 \cdot 7H_2O$ (Acros Organics, France) and $CaCl_2 \cdot 2H_2O$ (Cooper, France) was linear in the range from 0.5 to 50 $mg \cdot L^{-1}$ for Mg^{2+} and Ca^{2+} (R^2 = 0.999). The limits of detection (LOD) and quantification (LOQ) were 0.15 and 0.5 $mg \cdot L^{-1}$, respectively. All results of analyses were converted into molar concentrations.

Statistical analysis

Results were following a normal distribution and the variances of pairs of data sets were equal. Absorbed amounts from various formulations were compared using an appropriate Student *t*-test. Significance level was set at $p < 0.05$.

Results and discussion

Skin absorption profiles of Mg^{2+} and Ca^{2+} from three types of emulsions (O/TSW, TSW/O/W, TSW/O) and liposome suspensions composed of saturated and unsaturated phospholipids were investigated. The concentrations of Mg^{2+} and Ca^{2+} present in the aqueous phase were kept constant (2.7 and 8.0 $mmol \cdot kg^{-1}$ respectively). All 3 emulsion types were prepared using PEG-free emulsifiers based on vegetable-based raw materials at the concentration of 5% *m/m* in the final product. The choice of emulsifiers was dictated by the current trends in the cosmetic market towards products of natural origin. PGPR is a lipophilic (HLB = 1.5) nonionic emulsifier for W/O emulsions that is widely used in food products [39] and is recently entering the personal care industry. It is also known to be used in case of further introducing the primary W/O emulsion into a multiple emulsion (W/O/W) [40]. Thus, it allowed preparation of TSW/O/W emulsion based on the recipe of single TSW/O emulsion with high TSW content. G-CLLO was chosen as a hydrophilic emulsifier (HLB = 11) for the stabilization of O/TSW emulsion and the secondary emulsion of TSW/O/W system [41].

Liposomes were prepared by thin layer rehydration technique followed by sonication leading to formation of unilamellar vesicles. Saturated and unsaturated lipids (LPM-90H and LPM-90G respectively) were used because of their different penetration enhancement potentials that have been reported previously [42].

Physicochemical characterizations of all formulations are reported in Table III. Cryo-TEM observations of liposomes showed a collection of small unilamellar vesicles (Fig. 1). Their mean size was smaller than 100 nm. Aggregation of phosphatidylcholine vesicles by divalent cations like Mg^{2+} or Ca^{2+}, was not observed, which was in agreement with Düzgüneş *et al.* who did not notice aggregation or fusion of vesicles up to 10 mM Ca^{2+} and 100 mM NaCl [43]. Optical microscopy allowed observation of the 3 emulsion types (Fig. 1). Single emulsions showed well-separated spherical droplets with a mean diameter in the 1-2 µm range from the pictures. The TSW/O/W double emulsion showed larger droplets including smaller droplets of TSW inside their oil core. The O/TSW emulsions was quite fluid (twice the viscosity of pure water), which was expected for a well-stabilized emulsion containing 40% dispersed phase (MCT + G-CLLO). The TSW/O/W double emulsion was more viscous owing to its higher volume fraction of dispersed phase reaching 55% (50% primary TSW/O emulsion + 5% G-CLLO). These results show that the G-CLLO emulsifier was quite efficient at the stabilization of emulsions, so that droplets of dispersed phase were independent of each other. The viscosity of the TSW/O emulsion was quite high (about 7 times that of pure MCT oil) because of the fairly high concentration of dispersed phase (TSW + PGPR) of 65% approaching the theoretical limit for random packing of hard spheres.

Table III. Physicochemical characterisation of liposomes made of saturated and unsaturated phospholipids (LPM-90H and LPM-90G respectively) and 3 emulsion types: O/TSW, TSW/O/W and TSW/O. Mean size of emulsion droplets was estimated from optical microscopy observations; those of liposomes were measured by dynamic light scattering.

	LPM-90H	LPM-90G	O/TSW	TSW/O/W	TSW/O
Size (µm)	0.09	0.08	1-2	5-20	1-2
Viscosity (mPa·s) T = 25°C, strain rate = 300 s^{-1}	---	---	1.6 ± 0.1	6.8 ± 0.3	197 ± 13
pH	7.5	7.6	5.3	5.5	---

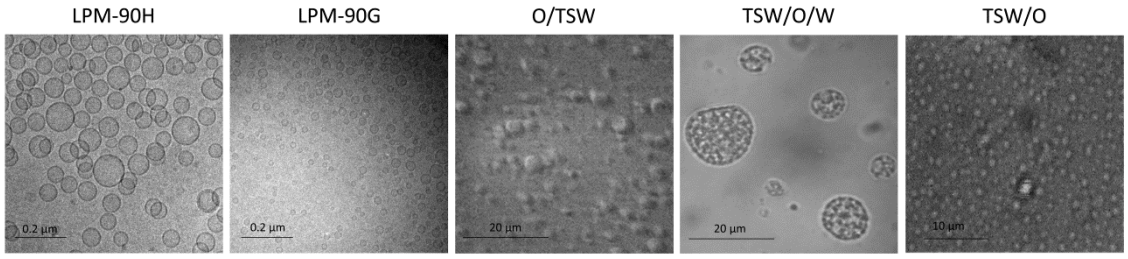

Figure 1. Microscopic images of formulations. Pictures of LPM-90H and LPM-90G were taken by cryo-TEM. Optical microscopy pictures were taken for O/TSW, TSW/O/W and TSW/O.

Skin absorption studies were performed by exposure of skin explants for 24 h under infinite dose conditions. These are not "in-use conditions" but they were chosen to maximize the effects of applied dose and allow clearer differentiation between endogenous and exogenous cations. Figure 2 and Table IV show the total absorbed amounts of Ca^{2+} and Mg^{2+} in AM + D + VE + SC (Q_{abs} in nmol·cm^{-2}) and their distribution in skin layers and AM. It can be noticed that the Q_{abs} of Ca^{2+} was higher than the one of Mg^{2+}, which was expected based on the composition of TSW. Moreover, skin absorption profiles differed depending on the also formulation type. Statistically significant differences were difficult to obtain which is related to the variability typical for the results of skin absorption experiments.

Q_{abs} values were generally not altered by incorporation of TSW in various formulations except for Mg^{2+}, loaded in LPM-90G and TSW/O which led to significantly lower Q_{abs}. Actually, in the

case of Ca^{2+} a trend to higher Q_{abs} was observed after application of LPM-90H and TSW/O/W and a lower Q_{abs} in the case of the O/TSW emulsion, but these differences were not statistically significant. Further analysis of Ca^{2+} distribution in the skin layers after 24 h exposure revealed a strong correlation between the Q_{abs} values and the amounts extracted from dermis for the LPM-90H and TSW/O/W formulations (Table IV). The same observation can be made for Mg^{2+} when loaded in TSW/O/W emulsion. We can therefore conclude from the results shown in Figure 2 that the application of a direct double emulsion led to significantly stronger retention of both cations within this layer as compared to control.

The mean amounts of calcium reaching AM followed the order in which the lipophilic character of formulations increased: TSW60% > Liposomes > TSW/O/W > O/TSW >TSW/O which was an expected result. Calcium and magnesium did not permeate from the TSW/O emulsion where TSW was entrapped in the inner core of the droplets. These results were also expected since it is well-known that the continuous lipophilic phase delays penetration of hydrophilic drugs (glucose [31], caffeine [44]) due to their unfavourable partition coefficient between oil and water that retains them in the inner aqueous droplets of W/O emulsions. However, a more surprising result was obtained for O/TSW in case of which Mg^{2+} was not recovered in the acceptor medium at all and calcium reached the AM in a very low amount. Even though O/TSW was the only emulsion in which TSW was not encapsulated and the concentrations of Ca^{2+} and Mg^{2+} in the external aqueous phase were higher than in the control, the absorption rates of both cations tended to be lower with high recovery from upper skin layers. An explanation is the higher oil fraction in these single emulsions comparatively to the other formulations; such oil can deposit on the skin surface and cause occlusion regardless the type of emulsion (O/W or W/O) and slow down the cation release. The main difference between both cations is their concentration being 3-fold higher for calcium than magnesium. This can explain why some

detectable calcium amount reaches the AM comparatively to magnesium during the time of the experiment.

Finally, the distribution of Ca^{2+} in the SC and VE did not differ significantly among the vehicles except for the O/TSW in the latter layer for both cations. This was the result of previous observation: the lowest total amount of cations absorbed from O/TSW (Fig. 2 and Table IV).

As it can be noticed from these results, separate Mg^{2+} and Ca^{2+} cations do permeate through skin, in spite of the electrostatic barrier against permeation of the positively charged (at low pH) *stratum corneum* (Table IV, Fig. 2). This is in agreement with several authors who reported the permeation of these inorganic cations in spite of their unfavourable physicochemical properties [11, 12, 45]. Both Mg^{2+} and Ca^{2+} are classified as kosmotrope cations in the framework of Hofmeister series. They are considered as hard metal ions of low polarizability because they retain valence electrons close to their nucleus. Hard cations can easily associate with hard bases bearing oxygen (e.g. water), nitrogen (e.g. amines, ammonia) and phosphate. Their strong interactions with water molecules can break water-water hydrogen bonds around them [46]. Therefore, their penetration in the lipophilic *stratum corneum* is considered less favourable as compared to chaotrope ions. The latter are more lipophilic as they can bind to lipids of the *stratum corneum* and accumulate in this layer. An extended literature reports that divalent cations easily bind to glycolipids, phospholipids, carboxylate, phosphate groups and carbonyl groups of *sn-2* phospholipid chains [47–50]. Moreover, their ability to permeate skin samples may be explained by the long exposure time and hydration of the skin during the course of the experiment, water being a penetration enhancer for hydrophilic substances in some parts of the *stratum corneum*. Van Hal *et al.* observed a water swelling of corneocytes and a smoother structure of the intercellular bilayers with the presence of water pools for skin explants immersed in PBS for 48 h. This may shorten the length of diffusional path in the *stratum corneum* between corneocytes. Additionally, small hydrophilic substances may profit from the presence

of water in the intercellular layer to diffuse [51–53]. Kosmotrope ions being strongly hydrated and tightly bound to water may benefit from skin hydration to cross the *stratum corneum*. Even though water creates water pools in the *stratum corneum* after long exposure time, a part of the *stratum corneum* does not participate in water pools formation. Thus, this deeper region over which lipid lamellae are formed still acts as a barrier [52]. Given the cosmetic application of TSW-based formulations and their specific action on skin barrier enhancement, the ideal formulation would enhance retention of Ca^{2+} and Mg^{2+} within *stratum corneum* and viable epidermis that are the target sites for this mechanism [15, 19]. This desired retention enhancement, however should be equal for both cations otherwise the initial Ca^{2+}:Mg^{2+} ratio (3:1) can change and lead to a reversed effect of inhibition of skin recovery, as reported in [15]. Considering the total quantity retained in skin, the Ca^{2+}:Mg^{2+} ratio was comprised between 1.8 and 3.4 depending on the formulation (Table IV) and, so far it was not different of the initial 3:1 ratio reported in TSW (Table I). This result is in agreement with previous papers showing a clear correlation between the concentration of ions and their flux [10, 12]. However, a closer observation of the results in the skin layers show that the ratios differ depending on the formulations.

In the upper epidermal layers, where the cations influence the skin repair mechanisms, some differences in their distribution arise depending on the formulations. In the *stratum corneum*, the increase in the ratio recovered from the skin layers was caused by the variations in Mg^{2+} as the values recovered for Ca^{2+} were comparable among all the formulations. Consequently, it was the dermal absorption of Mg^{2+} that drove the Ca^{2+}:Mg^{2+} ratios in this layer (Fig. 3). The ratio for the classical emulsions was equal to 1.5 and 9.5 in the *stratum corneum* respectively for the O/TSW and TSW/O. In the viable epidermis the ratio was very far from the 3:1 ratio. It was larger than 7 in the viable epidermis regardless the type of emulsion. It reached 19 for the TSW/O emulsion. High Ca^{2+}:Mg^{2+} ratios were recorded in viable epidermis precisely for the formulations

that tended to slow down the absorption of Mg^{2+}. It is worth noticing that in the experimental setup applied within this study, ion transport in viable skin layers occurs through ion-specific transporters [54, 55]. Physiological manifestation of this phenomena is the regulation of the ratio in the deeper layers in the absence of skin damage [56]. It can be hypothesized that when skin absorption is slow (TSW/O and O/TSW), the ion channels and ion transporters are efficient enough to pump the cations into deeper skin layers according to their concentration gradient. Observed low concentrations of Mg^{2+} in viable epidermis could be attributed to the efficacy of this mechanism. On the other hand, accumulation of Mg^{2+} could occur in VE for the formulations which accelerated skin absorption as a result of saturation of these ion transporters.

Liposomes have been chosen as vehicles due to their various benefits in skin delivery. Several authors observed increased skin absorption of molecules from liposome suspensions as compared to control solutions. Higher penetration rates were reported for the compositions including unsaturated phospholipids [42, 57]. Our results obtained for both types of liposomes were quite at variance with expectations based on literature data. In the present study, only slight enhancement of Ca^{2+} absorption was observed from LPM-90H liposomes, while LPM-90G did not promote absorption of Ca^{2+} and even delayed significantly the Mg^{2+} release into deep skin layers. The reason for the disagreement between our results and those reported in the literature is probably the different nature of tested molecules. Hydrophilic organic compounds, such as caffeine, do not interact with the lipids of the formulation and the penetration enhancement reported for this molecule is due to the ability of phosphatidylcholine to modulate skin barrier properties [42]. In present study, divalent cations contained in a multi-ionic mixture of TSW can interact with phospholipid bilayers since they can bind to phosphate groups [58, 59]. Alsop *et al.* demonstrated that Ca^{2+} and Mg^{2+} can bind to completion to the phospholipid membranes and that they are located inside the bilayer. Mg^{2+} was found to bind closer to the phosphate group and to coordinate with water-oxygen, while Ca^{2+} was adjacent to the glycerol

group [60]. Such a deep penetration of ions into the polar regions of the membrane led to swelling by water revealed by an increase of the lamellar repeat distance. The origin may be the electrical charging coming from divalent cation bonding that cause an electrostatic repulsion between bilayers together with the water uptake by hydration of bound cations [61]. Some authors reported that an increase in the number of water molecules bound per lipid molecule can better explain the swelling phenomena in the following order $Fe^{2+} > Mg^{2+} > Ca^{2+} > Zn^{2+}$, corresponding to the Hofmeister series [60]. For dipalmitoylphosphatidylcholine (DPPC), swelling has been reported until a ratio DPPC:Ca^{2+} = 1:0.14 mol/mol as in the present study [62]. The release of magnesium is greatly affected when Mg^{2+} is entrapped in both liposomes comparatively to calcium. Therefore, we observed an unbalance of Ca^{2+}:Mg^{2+} in the SC and VE with Ca^{2+}:Mg^{2+} ratios larger than 10.

The consequences of a disequilibrium in calcium to magnesium ratio > 2.6–2.8 or < 2 in humans has been recently reviewed by Rosanoff *et al.* [63]. Unbalanced dietary intake of these two ions was shown to have serious health consequences. For example, increased serum Ca^{2+}:Mg^{2+} ratio was associated with an increased risk of prostate or colorectal cancer [63]. Lee *et al.* have shown that high concentrations of Ca^{2+} associated with low Mg^{2+} and can result in a detrimental effect in the brain and suggested that administration of Mg^{2+} could be an strategy for reducing neuroinflammation caused by elevated Ca^{2+} in degenerative neurological disorders [64].

The single formulation which was in line with the initial value 3:1 and preserved it in all skin layers was the TSW/O/W double emulsion. This formulation maintained this initial ratio in SC which was not the case even for the control.

TSW/O/W had a specific behaviour where a part of cations reached the acceptor medium. The double emulsion in the paper by Ferreira *et al.* [31] had an intermediate glucose release profile ranging between those of the o/w and the w/o emulsions. In this study, the TSW/O/W promoted the absorption of both cations and even a fraction of Mg^{2+} was recovered in the acceptor

medium which was not the case for simple emulsions. This can be explained by the fact that this double emulsion combines both hydrophilic and hydrophobic emulsifiers (HLB of the mixture being close to 5) that interacts better with the lipidic fraction of *stratum corneum* than individual emulsifiers in simple emulsions. Such a mixture can act as a skin absorption enhancer.

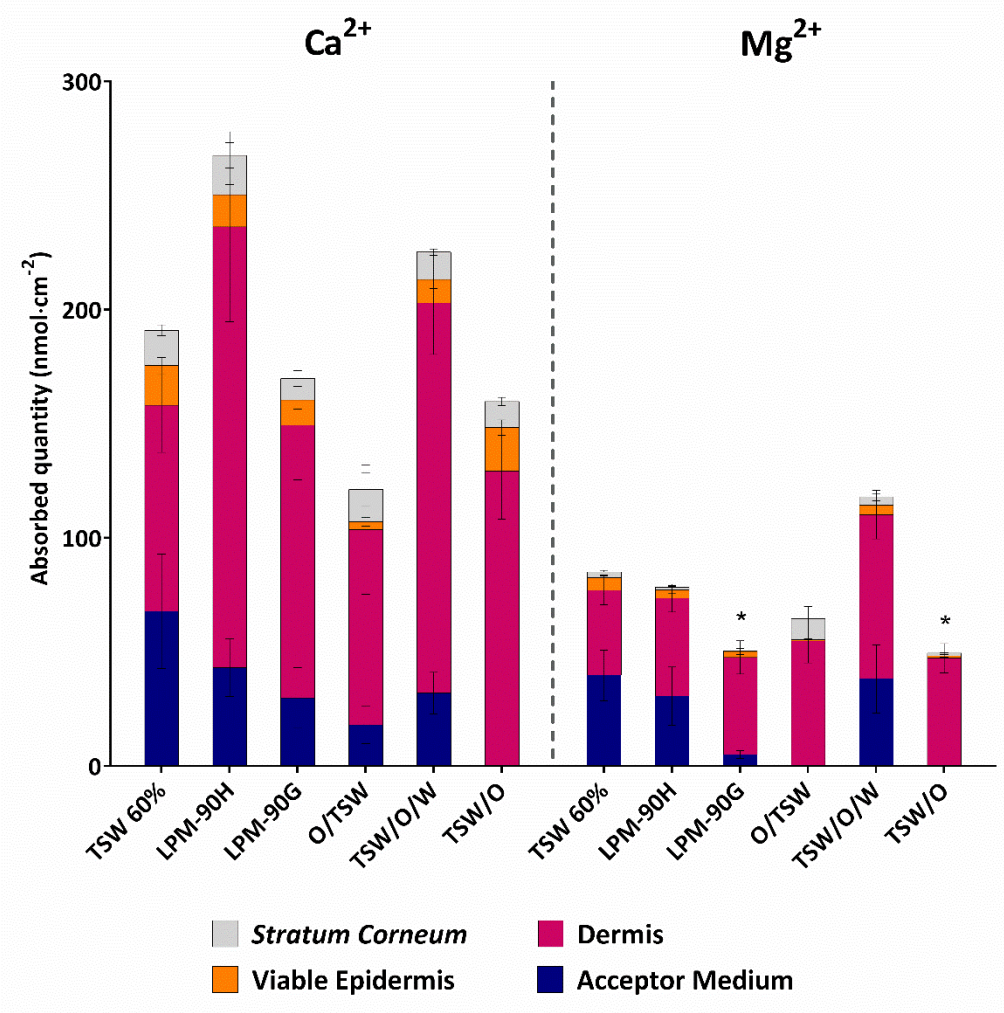

Figure 2. Distribution of Ca^{2+} and Mg^{2+} in the skin layers after 24 h exposure to formulations or TSW 60% as reference. Superposed bars correspond to total absorbed amount (Q_{abs}) Values represent *mean* ± *sem* from 8 experiments. Asterisk (*) indicates statistically significant difference obtained between given sample and TSW 60% in the *t*-test ($p < 0.05$).

Table IV. Results of dermal absorption of Ca^{2+} and Mg^{2+} from the emulsions and liposomes in nmol·cm^{-2}. Values represent *mean* ± *sem*. Ca^{2+}:Mg^{2+} ratios (*R*) were calculated based on the mean values obtained for each skin layer. The values being significantly different (*p > 0.05* in *t-test*) than the ones obtained for TSW 60% are framed in red when lower than for TSW 60%, and in green when higher than for TSW 60%.

	TSW 60%			**LPM-90H**			**LPM-90G**			**O/TSW**			**TSW/O/W**			**TSW/O**		
	Ca^{2+}	Mg^{2+}	***R***	Ca^{2+}	Mg^{2+}	***R***	Ca^{2+}	Mg^{2+}	***R***	Ca^{2+}	Mg^{2+}	***R***	Ca^{2+}	Mg^{2+}	***R***	Ca^{2+}	Mg^{2+}	***R***
Q_{abs}	190 ± 38.5	84± 11	**2.3**	267 ± 53	78 ± 20	**3.4**	169 ± 27	50 ± 7.4	**3.4**	117 ± 41	66 ± 16	**1.8**	171 ± 23	72 ± 11	**2.4**	160 ± 22	50 ± 6	**3.2**
AM	68 ± 25	40 ± 11	**1.7**	43 ± 13	31 ± 13	**1.4**	30 ± 13	5.0 ± 1.7	**6.0**	18 ± 8	0	**/**	32 ± 9	38 ± 15	**0.8**	0	0	**/**
D	90 ± 21	37 ± 6	**2.4**	193 ± 42	43 ± 6	**4.5**	120 ± 24	55 ± 7	**2.2**	86 ± 28	55 ± 9.6	**1.6**	171 ± 23	72 ± 10	**2.4**	129 ± 21	47 ± 6	**2.7**
VE	17 ± 4	5.5 ± 1	**3.0**	14 ± 4.5	3.6 ± 1.6	**3.9**	11 ± 3.9	2.6 ± 1.3	**4.2**	3.5 ± 2	0.5 ± 0.5	**7.0**	10 ± 4	4.2 ± 2	**2.4**	19 ± 3	1.0 ± 0.6	**19**
SC	15 ± 2	2.6 ± 0.7	**5.8**	17 ± 5.5	1.2 ± 0.7	**14.2**	9.4 ± 3.5	0.2 ± 0.2	**47**	14 ± 7	9.3 ± 5	**1.5**	12 ± 1	3.6 ± 1	**3.3**	11.4 ± 2	1.2 ± 0.1	**9.5**

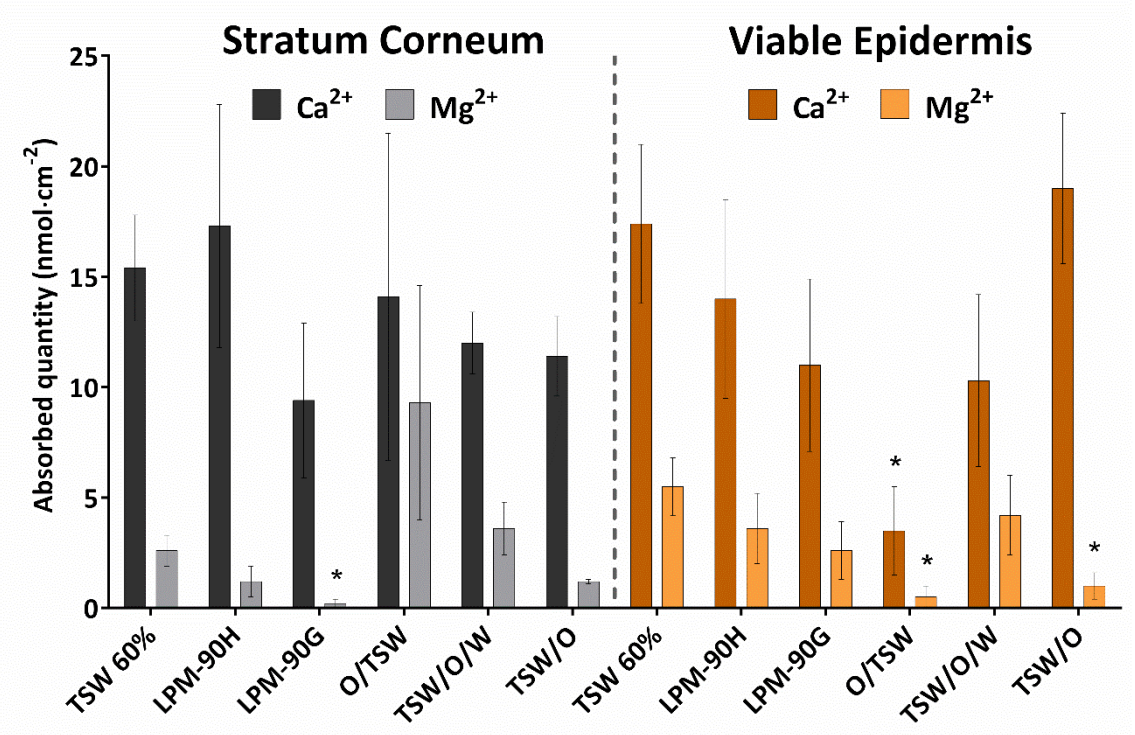

Figure 3. Distribution of Ca^{2+} and Mg^{2+} in the epidermal layers (SC and VE) after 24 h exposure. Values represent *mean* ± *sem* from 8 experiments. Asterisk (*) indicates statistically significant difference obtained between given sample and TSW 60% in the *t*-test ($p < 0.05$).

Conclusions

The present study aimed at investigating the impact of a vehicle, in which TSW was formulated, on skin absorption profiles of magnesium and calcium, the two cations of particular interest due to their biological activity in the skin tissue.

In the first place, we developed and characterised liposomal suspensions and concentrated emulsions (simple: water-in-oil, oil-in-water or double: water-in-oil-in-water) using vegetable raw material-derived emulsifiers. They were used as model formulations for skin absorption experiments.

We also confirmed that the beneficial effects of TSW, so far observed in cell culture of keratinocytes or fibroblasts, can occur in viable skin as ions constituting the mineral water are able to reach the different skin layers (SC, VE and D) from the TSW itself. Furthermore, the tests

performed on models of cosmetic formulations disclosed that ions can be released from the formulations and then penetrate into the skin. Liposomes, contrary to what has been reported for other molecules, did not enhance significantly skin absorption of Mg^{2+} but they improved the skin absorption profiles of Ca^{2+} leading to an unbalance of the Ca^{2+}:Mg^{2+} ratio. On the other hand, the TSW/O/W increased skin absorption (Q_{abs}) in case of both cations of interest as compared to control (TSW 60%), and it also respected the Ca^{2+}:Mg^{2+} ratio.

Acknowledgements

Authors are thankful to Pierre-Yves Dugas (University of Lyon 1, C2P2 UMR 5265) for cryo-TEM observations at the "Centre Technologique des Microstructures" (CTμ – University of Lyon 1). The help of Léon Bérard Medical Centre in providing skin explants is also acknowledged. Ministère de l'Enseignement Supérieur et de la Recherche (France) is also acknowledged for financial support of MT.

References

1. Masiero, S., Vittadini, F., Ferroni, C., Bosco, A., Serra, R., Frigo, A. C., Frizziero, A., The role of thermal balneotherapy in the treatment of obese patient with knee osteoarthritis. *Int. J. Biometeorol.* **62**, 243–252 (2018).
2. Yang, B., Qin, Q. zhong, Han, L. li, Lin, J., Chen, Y., Spa therapy (balneotherapy) relieves mental stress, sleep disorder, and general health problems in sub-healthy people. *Int. J. Biometeorol.* **62**, 261–272 (2018).
3. Jackson, R., Waters and spas in the classical world. *Med. Hist.* **34**, 1–13 (1990).
4. Gutenbrunner, C., Bender, T., Cantista, P., Karagülle, Z., A proposal for a worldwide definition of health resort medicine, balneology, medical hydrology and climatology. *Int. J. Biometeorol.* **54**, 495–507 (2010).
5. Huang, A., Seité, S., Adar, T., The use of balneotherapy in dermatology. *Clin. Dermatol.* **36**, 363–368 (2018).
6. Seite, S., Thermal waters as cosmeceuticals: La Roche-Posay thermal spring water example. *Clin. Cosmet. Investig. Dermatol.* **6**, 23–28 (2013).
7. Verhagen, A., Bierma-Zeinstra, S., Boers, M., Cardoso, J. R., Lambeck, J., De Bie, HCW, D. V.,

Balneotherapy (or spa therapy) for rheumatoid arthritis. *Cochrane Collab. Publ. by John Wiley Sons* (2015).

8. Nguyen, M., Revel, M., Dougados, M., Prolonged effects of 3 week therapy in a spa resort on lumbar spine, knee and hip osteoarthritis: follow-up after 6 months. A randomized controlled trial. *Br. J. Rheumatol.* **36**, 77–81 (1997).

9. Gambichler, T., Regeniter, P., Bechara, F. G., Orlikov, A., Vasa, R., Moussa, G., Stücker, M., Altmeyer, P., Hoffmann, K., Characterization of benign and malignant melanocytic skin lesions using optical coherence tomography in vivo. *J. Am. Acad. Dermatol.* **57**, 629–637 (2007).

10. Paweloszek, R., Briançon, S., Chevalier, Y., Gilon-Delepine, N., Pelletier, J., Bolzinger, M.-A., Skin absorption of anions: Part two. Skin absorption of halide ions. *Pharm. Res.* **33**, 1576–1586 (2016).

11. Bolzinger, M.-A., Bolot, C., Galy, G., Chabanel, A., Pelletier, J., Briançon, S., Skin contamination by radiopharmaceuticals and decontamination strategies. *Int. J. Pharm.* **402**, 44–49 (2010).

12. Chandrasekaran, N. C., Sanchez, W. Y., Mohammed, Y. H., Grice, J. E., Roberts, M. S., Barnard, R. T., Permeation of topically applied magnesium ions through human skin is facilitated by hair follicles. *Magnes. Res.* **29**, 35–42 (2016).

13. Waring, R. H., "Report on Magnesium Sulfate Across the Skin" (2014), (available at http://www.mgwater.com/transdermal.shtml).

14. de Ligt, R., van Duijn, E., Grossouw, D., Bosgra, S., Burggraaf, J., Windhorst, A., Peeters, P. A. M., van der Luijt, G. A., Alexander-White, C., Vaes, W. H. J., Assessment of dermal absorption of aluminum from a representative antiperspirant formulation using a ^{26}Al microtracer approach. *Clin. Transl. Sci.* **11**, 573–581 (2018).

15. Denda, M., Katagiri, C., Hirao, T., Maruyama, N., Takahashi, M., Some magnesium salts and a mixture of magnesium and calcium salts accelerate skin barrier recovery. *Arch. Dermatol. Res.* **291**, 560–563 (1999).

16. Lee, S. H., Elias, P. M., Feingold, K. R., Mauro, T., A role for ions in barrier recovery after acute perturbation. *J. Invest. Dermatol.* **102**, 976–979 (1994).

17. Mauro, T., Bench, G., Sidderas-Haddad, E., Feingold, K., Elias, P., Cullander, C., Acute barrier perturbation abolishes the Ca^{2+} and K^{+} gradients in murine epidermis: Quantitative measurement using PIXE. *J. Invest. Dermatol.* **111**, 1198–1201 (1998).

18. Menon, G. K., Price, L. F., Bommannan, B., Elias, P. M., Feingold, K. R., Selective obliteration of the epidermal calcium gradient leads to enhanced lamellar body secretion. *J. Invest. Dermatol.* **102**, 789–795 (1994).

19. Denda, M., Fuziwara, S., Inoue, K., Influx of calcium and chloride ions into epidermal keratinocytes regulates exocytosis of epidermal lamellar bodies and skin permeability barrier homeostasis. *J. Invest. Dermatol.* **121**, 362–367 (2003).

20. Denda, M., Hosoi, J., Asida, Y., Visual imaging of ion distribution in human epidermis. *Biochem. Biophys. Res. Commun.* **272**, 134–137 (2000).

21. Proksch, E., Nissen, H. P., Bremgartner, M., Urquhart, C., Bathing in a magnesium-rich Dead

Sea salt solution improves skin barrier function, enhances skin hydration, and reduces inflammation in atopic dry skin. *Int. J. Dermatol.* **44**, 151–157 (2005).

22. Schwartz, J. R., Marsh, R. G., Draelos, Z. D., Zinc and skin health: overview of physiology and pharmacology. *Dermatol. Surg.* **31**, 837–847 (2005).

23. Celerier, P., Litoux, P., Dreno, B., Richard, A., Modulatory effects of selenium and strontium salts on keratinocyte-derived inflammatory cytokines. *Arch. Dermatol. Res.* **287**, 680–682 (1995).

24. Suda, T., Suzuki, Y., Matsui, T., Inoue, T., Niide, O., Yoshimaru, T., Suzuki, H., Ra, C., Ochiai, T., Dapsone suppresses human neutrophil superoxide production and elastase release in a calcium-dependent manner. *Br. J. Dermatol.* **152**, 887–895 (2005).

25. Joly, F., Charveron, M., Ariès, M. F., Bidault, J., Kahhak, L., Beauvais, F., Gall, Y., Effect of Avène spring water on the activation of rat mast cell by substance P or antigen. *Skin Pharmacol. Appl. Skin Physiol.* **11**, 111–116 (1998).

26. Beauvais, F., Garcia-Mace, J. L., Joly, F., In vitro effects of Uriage spring water on the apoptosis of human eosinophils. *Fundam. Clin Pharmacol*. **12**, 446–450 (1998).

27. Otto, A., du Pleiss, J., Wiechers, J. W., Formulation effects of topical emulsions on transdermal and dermal delivery. *Int. J. Cosmet. Sci.* **31**, 1–19 (2009).

28. Sala, M., Diab, R., Elaissari, A., Fessi, H., Lipid nanocarriers as skin drug delivery systems: Properties, mechanisms of skin interactions and medical applications. *Int. J. Pharm.* **535**, 1–17 (2018).

29. El Maghraby, G. M., Barry, B. W., Williams, A. C., Liposomes and skin: From drug delivery to model membranes. *Eur. J. Pharm. Sci.* **34**, 203–222 (2008).

30. Ita, K. B., Du Preez, J., du Plessis, J., Lane, M. E., Hadgraft, J., Dermal delivery of selected hydrophilic drugs from elastic liposomes: effect of phospholipid formulation and surfactants. *J. Pharm. Pharmacol.* **59**, 1215–1222 (2007).

31. Ferreira, L. A. M., Seiller, M., Grossiord, J. L., Marty, J. P., Wepierre, J., Vehicle influence on in vitro release of glucose. *J. Control. Release* **33**, 349–356 (1995).

32. Mahrhauser, D., Nagelreiter, C., Baierl, A., Skipiol, J., Valenta, C., Influence of a multiple emulsion, liposomes and a microemulsion gel on sebum, skin hydration and TEWL. *Int. J. Cosmet. Sci.* **37**, 181–186 (2015).

33. Bangham, A. D., Hill, M. W., Miller, N. G. A., in *Methods in Membrane Biology*, E. D. Korn, Ed. (Plenum Press, New York, 1974), pp. 1–68.

34. Gray, G. M., Yardley, H. J., Lipid compositions of cells isolated from pig, human, and rat epidermis. *J. Lipid Res.* **16**, 434–440 (1975).

35. Wester, R. C., Melendres, J., Sedik, L., Maibach, H., Riviere, J. E., Percutaneous absorption of salicylic acid, theophylline, 2,4-dimethylamine, diethyl hexyl phthalic acid, and p-aminobenzoic acid in the isolated perfused porcine skin flap compared to man in vivo. *Toxicol. Appl. Pharmacol.* **151**, 159–165 (1998).

36. Paweloszek, R., Briançon, S., Chevalier, Y., Gilon-Delepine, N., Pelletier, J., Bolzinger, M.-A., Skin absorption of anions: Part one. Methodology for in vitro cutaneous absorption measurements. *Pharm. Res.* **33**, 1564–1575 (2016).

37. “OECD, Guidance Document for the Conduct of Skin Absorption Studies” (2004).

38. Tarnowska, M., Briançon, S., Resende De Azevedo, J., Chevalier, Y., Barratier, C., Pourcher, T., Bolzinger, M.-A., Formulation of survival acceptor medium able to maintain the viability of skin explants over in vitro dermal experiments. *Int. J. Cosmet. Sci.* accepted (2019).

39. Bastida-Rodríguez, J., The food additive polyglycerol polyricinoleate (E-476): Structure, applications, and production methods. *ISRN Chem. Eng.* **2013**, 1–21 (2013).

40. Eisinaite, V., Duque, P., Schroën, K., Berton-Carabin, C., Tayloring W/O/W emulsion composition for effective encapsulation: The role of PGPR in water transfer-induced swelling. *Food Res. Int.* **106**, 722–728 (2018).

41. Blume, G., Carrier system for the transport of active substances into the skin. US 9211238B2 (2015).

42. Kim, C., Shim, J., Han, S., Chang, I., The skin-permeation-enhancing effect of phosphatidylcholine: caffeine as a model active ingredient. *J. Cosmet. Sci.* **53**, 363–374 (2002).

43. Düzgüneş, N., Ohki, S., Calcium-induced interaction of phospholipid vesicles and bilayer lipid membranes. *Biochim. Biophys. Acta* **467**, 301–308 (1977).

44. Briançon, S., Chevalier, Y., Bolzinger, M.-A., Biopharmaceutical evaluation of various dosage forms intended for caffeine topical delivery. In *Advances in Dermatological Sciences*, Chilcott, R., Brain, K. R., Eds. (Issues in Toxicology No 20, RSC Publishing, Cambridge), pp. 88–100 (2013).

45. Youenang Piemi, M. P., Korner, D., Benita, S., Marty, J.-P., Positively and negatively charged submicron emulsions for enhanced topical delivery of antifungal drugs. *J. Control. Release* **58**, 177–187 (1999).

46. Okur, H. I., Hladílková, J., Rembert, K. B., Cho, Y., Heyda, J., Dzubiella, J., Cremer, P. S., Jungwirth, P., Beyond the Hofmeister series: Ion-specific effects on proteins and their biological functions. *J. Phys. Chem. B* **121**, 1997–2014 (2017).

47. Melcrová, A., Pokorna, S., Pullanchery, S., Kohagen, M., Jurkiewicz, P., Hof, M., Jungwirth, P., Cremer, P. S., Cwiklik, L., The complex nature of calcium cation interactions with phospholipid bilayers. *Sci. Rep.* **6**, 1–12 (2016).

48. Böckmann, R. A., Grubmüller, H., Multistep binding of divalent cations to phospholipid bilayers: A molecular dynamics study. *Angew. Chem. Int. Ed.* **43**, 1021–1024 (2004).

49. Koshy, K. M., Wang, J., Boggs, J. M., Divalent cation-mediated interaction between cerebroside sulfate and cerebrosides: An investigation of the effect of structural variations of lipids by electrospray ionization mass spectrometry. *Biophys. J.* **77**, 306–318 (1999).

50. Rojanasakul, Y., Wang, L. Y., Bhat, M., Glover, D. D., Malanga, C. J., Ma, J. K. H., The transport barrier of epithelia: A comparative study on membrane permeability and charge selectivity in the rabbit. *Pharm. Res.* **9**, 1029–1034 (1992).

51. Ogawa-Fuse, C., Morisaki, N., Shima, K., Hotta, M., Sugata, K., Ichihashi, T., Oguri, M., Yoshida, O., Fujimura, T., Impact of water exposure on skin barrier permeability and ultrastructure. *Contact Dermatitis* **80**, 228–233 (2019).

52. Warner, R. R., Stone, K. J., Boissy, Y. L., Hydration disrupts human stratum corneum

ultrastructure. *J. Invest. Dermatol.* **120**, 275–284 (2003).

53. van Hal, D. A., Jeremiasse, E., Junginger, H., Spies, F., Bouwstra, J. A., Structure of fully hydrated human stratum corneum: a freeze-fracture electron microscopy study. *J. Invest. Dermatol.* **106**, 89–95 (1996).

54. Penner, R., Fasolato, C., Hoth, M., Calcium influx and its control by calcium release. *Curr. Opin. Neurobiol.* **3**, 368–374 (1993).

55. Sahni, J., Scharenberg, A. M., Editor, G., Hediger, M. A., The SLC41 family of MgtE-like magnesium transporters q. *Mol. Aspects Med.* **34**, 620–628 (2013).

56. Koegel, H., Alzheimer, C., Expression and biological significance of Ca^{2+}-activated ion channels in human keratinocytes. *FASEB J.* **15**, 145–154 (2001).

57. Touitou, E., Levi-Schaffer, F., Dayan, N., Alhaique, F., Riccieri, F., Modulation of caffeine skin delivery by carrier design: liposomes versus permeation enhancers. *Int. J. Pharm.* **103**, 131–136 (1994).

58. Puskin, J. S., Divalent cation binding to phospholipids: An EPR study. *J. Membr. Biol.* **35**, 39–55 (1977).

59. Ohki, S., Düzgünes, N., Divalent cation-induced interaction of phospholipid vesicle and monolayer membranes. *Biochim. Biophys. Acta - Biomembranes* **552**, 438–449 (1979).

60. Alsop, R. J., Maria Schober, R., Rheinstädter, M. C., Swelling of phospholipid membranes by divalent metal ions depends on the location of the ions in the bilayers. *Soft Matter* **12**, 6737–6748 (2016).

61. Binder, H., Zschörnig, O., The effect of metal cations on the phase behavior and hydration characteristics of phospholipid membranes. *Chem. Phys. Lipids* **115**, 39–61 (2002).

62. Kučerka, N., Dushanov, E., Kholmurodov, K. T., Katsaras, J., Uhríková, D., Calcium and zinc differentially affect the structure of lipid membranes. *Langmuir* **33**, 3134–3141 (2017).

63. Rosanoff, A., Dai, Q., Shapses, S. A., Essential nutrient interactions: Does low or suboptimal magnesium status interact with vitamin D and/or calcium status? *Adv. Nutr.* **7**, 25–43 (2016).

64. Lee, A. H., Nikraz, H., BOD:COD ratio as an indicator for river pollution. *Int. Proc. Chem. Biol. Environ. Eng.* **51**, 139–142 (2015).